

# Gas mixing in microchannels using the direct simulation Monte Carlo method

Moran Wang<sup>a,b</sup>, Zhixin Li<sup>a,\*</sup>

<sup>a</sup> Department of Engineering Mechanics, Tsinghua University, Beijing 100084, PR China

<sup>b</sup> Department of Mechanical Engineering, The Johns Hopkins University, Baltimore, MD 21218, USA

Received 6 April 2005; received in revised form 15 July 2005

Available online 13 December 2005

## Abstract

Mixing in microchannels is an important problem because the flow is always laminar flow even though the velocity may be high. The present paper analyzes the inherent factors affecting micro gas mixing using the direct simulation Monte Carlo (DSMC) method at high Knudsen numbers. The discretization errors in the DSMC method were analyzed to ensure numerical accuracy. The simulation results show that the wall characteristics have little effect on the mixing length when the main gas flow velocities for different wall characteristics were the same. The mixing length is nearly inversely proportional to the gas temperature. The dimensionless mixing coefficient, which is the ratio of the mixing length to the channel height, is proportional to the Mach number and inversely proportional to the Knudsen number. This conclusion was validated for microscale gas flows, but is expected to apply to all laminar gas flows at all scales.

© 2005 Elsevier Ltd. All rights reserved.

## 1. Introduction

Adequate mixing is a problem in MEMS/NEMS devices due to the small characteristic size for which the flows are always laminar [9,8,13]. Gas mixing studies are an essential requirement for the design of propulsion devices in Power-MEMS [15,18]. The degree of mixing has been shown to greatly affect chemical reaction rates and gas-fuel combustion efficiencies [12]. For this reason, the mixing process in continua has been intensely studied both for supersonic and subsonic shear layers [5,26]. However, in microchannels, the continuum assumption may break down due to the high Knudsen number caused by the small characteristic length, even though the gas may not be really rarefied [6].

Because the continuum assumption may not apply, the Boltzmann and molecular dynamics based methods are

the only choices for analyzing high Knudsen number gas flows. The direct simulation Monte Carlo (DSMC) method [3], probably the most successful method, was used initially for dilute gas flows and now is often applied to simulate micro gas flows [14,21,22,25]. Yan and Farouk [27] may have been the first ones to simulate gas mixing in microchannels using the DSMC method. They studied two parallel gas streams driven by inlet–outlet pressure differences. They found that the mixing decreased with increasing inlet–outlet pressure difference and that the mixing process for nearly specularly-reflective walls was much slower than that for completely diffuse walls. The mixing length for a nearly specularly-reflective wall might be  $O(10)$  times that for a completely diffuse wall. In their simulations, both the inlet pressure and the incoming gas velocity were set at the inlet with the outlet having unspecified boundary conditions. In our opinion, the inlet–outlet pressure difference and the wall characteristics may affect the flow but do not directly affect the mixing process. Gas mixing in microchannels is mainly due to the relationship between the flow characteristics and the gas properties.

\* Corresponding author. Tel.: +86 10 6277 2919; fax: +86 10 6278 1610.  
E-mail addresses: [moralwang@jhu.edu](mailto:moralwang@jhu.edu) (M. Wang), [lizhx@tsinghua.edu.cn](mailto:lizhx@tsinghua.edu.cn) (Z. Li).

## Nomenclature

$D$	gas diffusion coefficient	$k$	Boltzmann constant
$H$	channel height	$l_{\text{mix}}$	mixing length
$R$	gas constant	$m$	gas molecular mass
$Kn$	Knudsen number	$\gamma$	specific heat ratio
$Ma$	Mach number	$\eta_{\text{mix}}$	dimensionless mixing coefficient
$T$	gas temperature	$\rho$	gas density
$T_{\text{ref}}$	reference temperature	$\sigma$	gas molecular diameter
$V$	gas mean velocity	$\zeta$	internal energy degrees of freedom
$d_{\text{ref}}$	reference molecular diameter	$\omega$	viscosity–temperature index
$n$	molecular number density		

In this paper, the mixing of two-component gas streams was investigated using DSMC codes developed for micro geometries and different boundary conditions. The analyses simulated two parallel gas streams entering a microchannel separated by a splitter plate for various working conditions. The effect of the wall characteristics was also examined. Various inlet gas velocities (50–200 m/s) and gas temperatures (200–400 K) were simulated to show their influences on the mixing process.

## 2. Numerical methods

### 2.1. DSMC method

DSMC is a molecular-based statistical simulation method for rarefied gas flows introduced by Bird [3]. The method numerically solves the dynamic equations for the gas flow using thousands of simulated molecules. Each simulated molecule represents a large number of real molecules. With the assumption of molecular chaos and a rarefied gas, only the binary collisions need be considered, and as a result the molecular motion and the collisions are uncoupled if the computational time step is smaller than the physical collision time. The interactions with boundaries and with other molecules conserve both momentum and energy. The macroscopic flow characteristics are obtained statistically by sampling the molecular properties in each cell.

At the beginning of the calculation, the simulated particles are uniformly distributed statistically in the cells. At each time step, all particles move according to their individual velocities, interact with the boundaries and are then indexed. A certain number of collision pairs are selected in each cell using the no-time-counter (NTC) method for the collision calculations. These steps are repeated to increase the sample size until the statistical errors are small enough. The DSMC method can simulate non-equilibrium and unsteady gas flows. A steady-state flow field is obtained with a sufficiently long simulation time. When the temperature is not too high (<1000 K) or too low ( $\geq 200$  K), the hard sphere model without intermolecular attractive potential is accurate enough for the collisions

[19,20,22,23]. The present simulations used the variable hard sphere (VHS) model [3].

The codes were developed based Bird's standard code (1994) and validated for various micro geometries and different boundary conditions [19,21]. All the current calculations were performed on a Beowulf cluster with 550 MHz CPUs. The sample size in each case included more than  $5 \times 10^6$  molecules, which provides an acceptable accuracy [17,24]. The CPU time for each typical case was over 150 h.

### 2.2. Discretization effects analysis

According to [3], only when the computational time step is less than the mean collision time can the molecular movements and collisions be decoupled. The cells are made small enough to restrict collisions with nearby particles but should contain a sufficient number of particles so that the method remains statistically accurate. Empirical results have shown that the cells should be no larger than one mean free path and should contain at least twenty particles. There was no theory for this until the Green–Kubo formalism was used to quantitatively evaluate the dependence of the gas transport properties on the cell size [1,2] and the time step [7,10]. However, these results made the simulation for long channel flows (with large  $L/H$ ) prohibitively expensive. In 2003, Ilgaz and Çelenligil [11] suggested that analyses can use cell sizes much greater than the local mean free paths in directions where the gradients of the flow properties are small and the time step could also be enlarged accordingly. Their comparison of the pressure distributions along a long channel for different cell sizes suggested that the results were accurate even for cell sizes 100 times the mean free paths. However, a detailed comparison showed that the enlarged cell size destroys the velocity and temperature field accuracies, even though the cell size effect on the pressure distribution is limited.

Fig. 1 compares the pressure distributions and velocity profiles for different cell sizes. For each case, the time step and molecule number satisfied Bird's requirements. The results in Fig. 1 may be disappointing, but they illustrate the discretization requirements for the DSMC simulation accuracy. Recently, Rader et al. [16] proposed

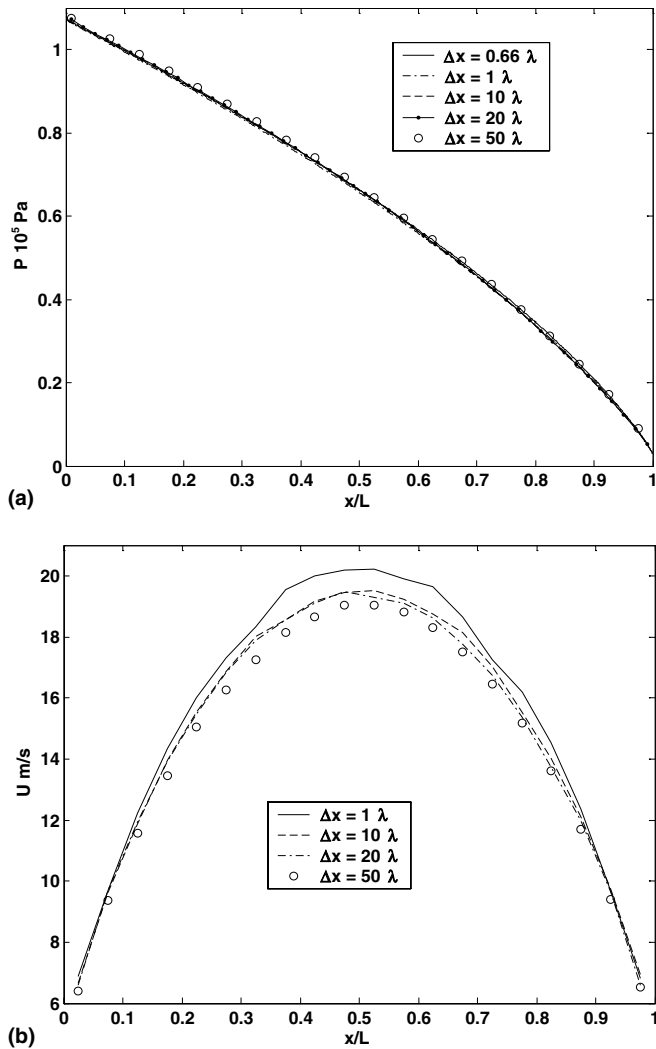


Fig. 1. Microchannel flow for different cell sizes. The channel was 50  $\mu\text{m}$  long and 1  $\mu\text{m}$  high. The inlet condition were atmospheric pressure and 300 K and the outlet was a vacuum. The wall was completely diffuse with  $T_{\text{wall}}$  at 300 K. The gas is nitrogen. (a) Pressure distributions along the channel; (b) velocity profiles at the channel mid-length.

independently a quantitative expression for the dependence of the thermal conductivity on the computational parameters, including time step, cell size, and particle number, which further confirms this conclusion.

The subcell technique, which Bird introduced into a standard DSMC code (1994), can be used to somewhat reduce the computational costs for large  $L/H$  channel flow simulations. Fig. 2 shows that, if the cell size cannot be reduced to less than the local mean free path due to computer limitations, the subcell technique provides an alternative as long as the subcell size, instead of the cell size, is smaller than the mean free path.

The following simulations use the subcell technique when necessary. In each case the cell (or subcell) size was always smaller than the local gas mean free path. The time step was then chosen as half of the smallest collision time in the channel. Each cell contained about twenty molecules, which ensures the accuracies of the simulations.

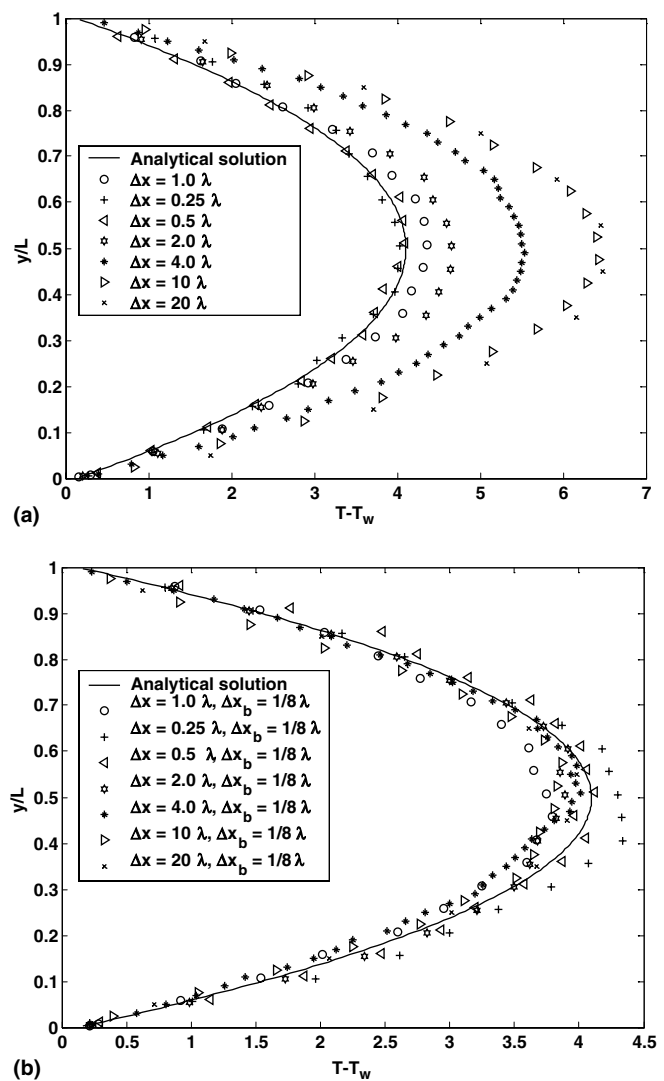


Fig. 2. Subcell effects on the simulation results. The flow is standard 1D Couette flow. The channel is 10  $\mu\text{m}$  wide. The initial state of the nitrogen gas is the standard state (1 atm and 273 K). The wall is completely diffuse and the wall temperature is 273 K. The analytical solution is from [4]. (a) Results without subcells; (b) results using the subcell technique.

### 3. Results and discussion

The geometry for the mixing of two different gases in a microchannel is illustrated in Fig. 3. The effect of density on the mixing was eliminated by choosing gases with the same molecular mass, CO and  $\text{N}_2$ . The two gas streams enter the channel separated by a splitter plate. The 2D channel is  $H$  in height and  $L$  in length.  $H$  is chosen as 1  $\mu\text{m}$  with  $L$  long enough for the mixing, as will be discussed in the following section. The entering gas temperature is 300 K. The splitter plate length is  $L/3$  or shorter. Both of its surfaces are fully specularly reflective. The channel walls are fully specularly reflective or completely diffuse with temperatures of 300 K. The gas properties used in the simulations are listed in Table 1 [3].

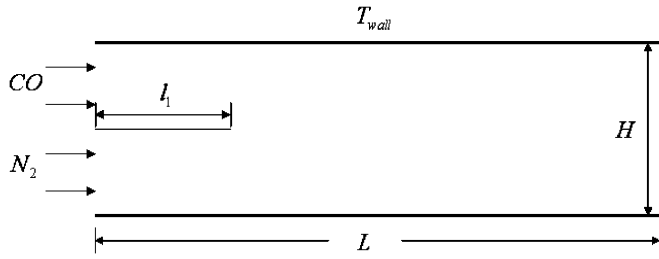


Fig. 3. Schematic of the mixing problem geometry and conditions.

Table 1

Gas properties

	$m$ ( $\times 10^{-26}$ kg)	$\zeta$	$d_{\text{ref}}$ ( $\times 10^{-10}$ m)	$T_{\text{ref}}$ (K)	$\omega$	$\gamma$
N <sub>2</sub>	4.65	2	4.17	273	0.74	1.4
CO	4.65	2	4.12	273	0.73	1.4

### 3.1. Wall effects

In Yan’s results (2002), the gas mixing was quite sensitive to the channel wall accommodation coefficient. The mixing length in a fully specularly-reflective-wall channel was  $O(10)$  times that in a completely diffuse-wall channel. Therefore, the wall effects on the mixing process were examined first.

Consider two microchannels with  $L/H$  equal to 10. One channel has completely diffuse walls with wall temperatures of 300 K. The other has fully specularly-reflective walls. The inlet number densities and the initial velocities are given and the outlet boundary is a vacuum. The gases in the channel are accelerated due to the inlet–outlet pressure difference with the main flow velocity increasing along the channel. The gas main flow velocity was defined at a plane gas beyond the splitter plate for the diffuse-wall case with this velocity then used as the inlet velocity to the specular-wall case, so that the two flows had almost the same main flow velocities for a reasonable comparison of the mixing process.

The mixing process are characterized by a mixing length as in [27], the mixing length is defined as the length for the two gases to be fully mixed. Yan and Farouk determined the mixing length by the density contours. The gases were considered full mixed when the density contours both appeared symmetric about the channel centerline. In practice, this method results in large errors since it is somewhat subjective. Here we use a quantitative determination of the mixing length. Using the densities near the walls when the gases are fully mixed in the channel, the densities near the upper and lower walls should be equal. Therefore, define the relative density difference

$$\xi = \frac{\Delta\rho}{\rho} = \frac{\rho_1 - \rho_0}{\rho_1} \quad (1)$$

where  $\rho_1$  refers to the denser side, and  $\rho_0$  refers to the diluter side to characterize the mixing process along the channel. The change in  $\xi$  along the channel should change

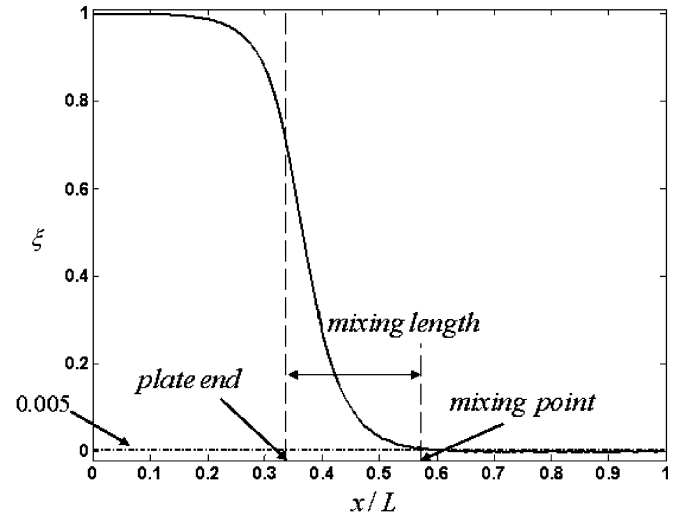


Fig. 4. Density difference evolution along the channel for determination of the mixing length. The dash-dotted line is at a value of  $\xi = 0.005$ .

asymptotically from 1 to 0. The critical value to judge where the gases are fully mixed was chosen as  $\xi = 0.5\%$ . Fig. 4 shows a typical determination of the mixing length from the simulation results.

For the completely diffuse-wall channel, the inlet densities of both gases were set to the densities for 0.5 standard atmosphere pressures with an initial inlet velocity of 300 m/s. The resulting main flow velocity leaving the splitter plate was about 74 m/s, which was then used in the fully specularly-reflective-wall channel as the inlet gas velocities. Thus, the main flow velocities of the gases during the mixing processes were very similar. The calculated mixing length for the diffuse-wall channel was 2.8  $\mu\text{m}$  and 2.5  $\mu\text{m}$  for the specular-wall channel. Even though the diffuse-wall characteristics made the velocity profiles and velocity evolution along the channel differ significantly from those in the specularly-reflective-wall channel, for similar main flow velocities, the mixing lengths were still similar.

### 3.2. Velocity effects

Since the effect of the wall characteristics on the mixing process was limited, the inlet–outlet pressure difference also did not significantly affect the gas mixing. However, the main flow velocity should play a more important role. Inlet main flow velocities from 50 to 200 m/s were considered for flow in the fully specularly-reflective-wall channel. The results shown in Fig. 5 show that the mixing length is almost proportional to the main flow velocity.

### 3.3. Temperature effects

The diffusion coefficient is known to be strongly dependent on the gas temperature. Fig. 6 shows the effect of temperature on the micro gas mixing for the fully specularly-reflective walls case. The inlet gas number densities were  $1.29 \times 10^{25}$  and the inlet velocities were 105.9 m/s.

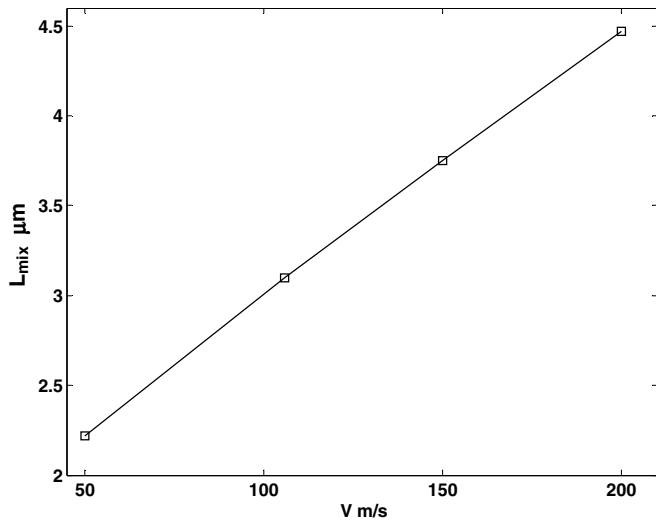


Fig. 5. Mixing length variation for various main flow velocities for  $T = 300$  K.

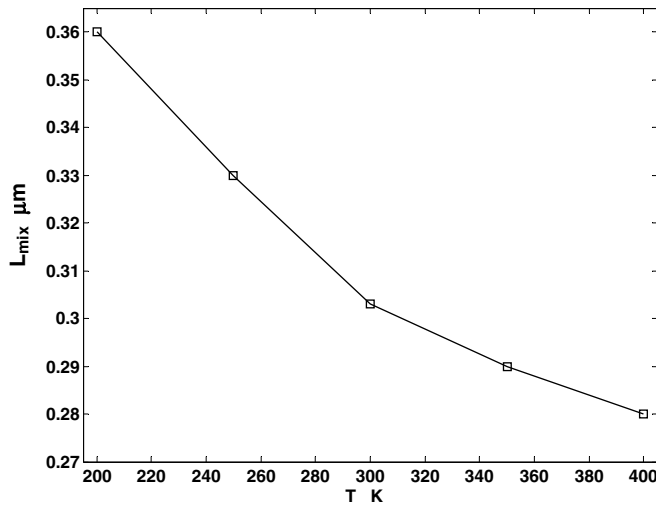


Fig. 6. Mixing length variation for various main flow temperatures for  $V = 106$  m/s.

The inlet temperatures ranged from 200 K to 400 K. The mixing length decreased with temperature, indicating the important of high temperatures for enhancing the gas mixing.

### 3.4. Dimensionless mixing coefficient

The calculations showed that the main flow velocity and temperature are the most important factors affecting the micro gas mixing. The wall characteristics affect the velocity and temperature profiles and distributions, but the effect on the mixing length is limited.

The two dimensionless parameters describing the micro gas flow are the Knudsen number and the Mach number [19,24],

$$Ma = \frac{V}{\sqrt{\gamma RT}} \quad (2)$$

$$Kn = \frac{1}{\sqrt{2} \pi n \sigma^2 H} \quad (3)$$

From molecular gas dynamics, the diffusion coefficient can be expressed as

$$D = \frac{3}{8n\sigma^2} \sqrt{\frac{kT}{\pi m}} \quad (4)$$

In laminar flow, the mixing process is mainly dependent on diffusion. Therefore, the channel length  $L_{mix}$  for complete mixing across a channel of height  $H$  is proportional to

$$L_{mix} \propto \frac{H^2 V}{D} \quad (5)$$

The dimensionless mixing coefficient can then be defined as the ratio of the mixing length to the channel height,

$$\eta_{mix} = \frac{L_{mix}}{H} \quad (6)$$

Combining Eqs. (2)–(6), the mixing coefficient can then be related to the two dimensionless parameters as

$$\eta_{mix} \propto \frac{Ma}{Kn} \quad (7)$$

Therefore, the mixing process is proportional to the Mach number and inversely proportional to the Knudsen number.

### 3.5. Knudsen number effects

Fig. 7 shows the effect of Knudsen number on the mixing coefficients for the fully specularly-reflective channel. The inlet gas Mach number was 0.3 while the Knudsen numbers ranged from 0.01 to 0.2. For  $Kn = 0.05–0.2$ , the channel aspect ratio was  $L/H = 10$ . For  $Kn = 0.02$ ,  $L/H = 20$  was used to eliminate the effect of the outlet on the mixing. For  $Kn = 0.01$ ,  $L/H = 30$  and the subcell technique was used to reduce the computational cost. For small Knudsen numbers ( $\leq 0.1$ ), the mixing coefficient,  $\eta_{mix}$ , is

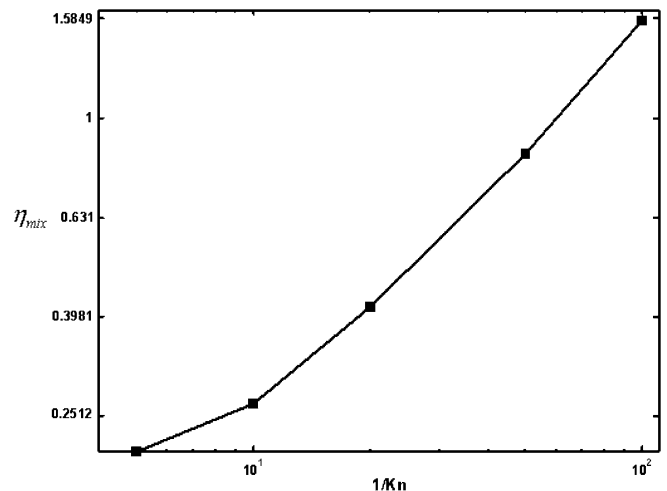


Fig. 7. Mixing coefficient variation for various Knudsen numbers at  $Ma = 0.3$ . Both axes are logarithmic.

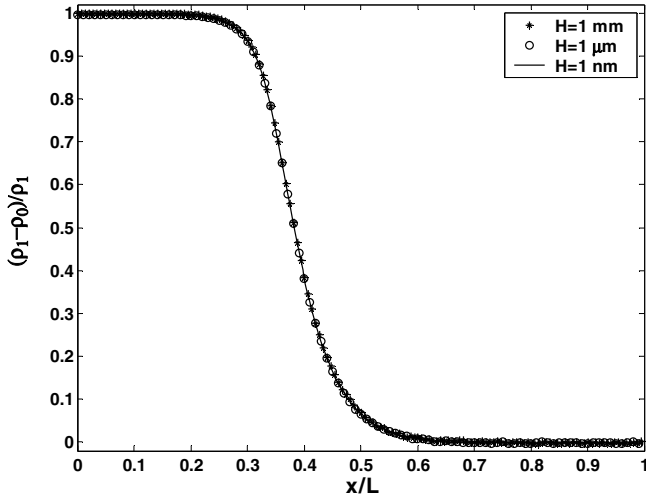


Fig. 8. Density difference profiles for various channel sizes for  $Kn = 0.1$  and  $Ma = 0.3$ .

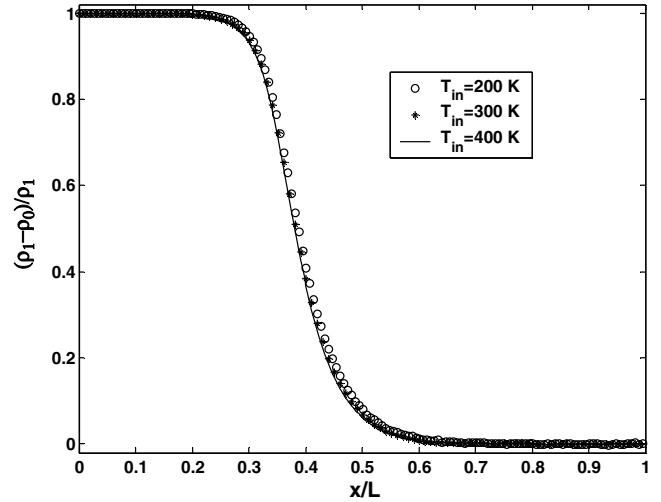


Fig. 10. Density difference profiles for various inlet gas temperature at  $Ma = 0.3$  and  $Kn = 0.1$ .

nearly linearly proportional to the reciprocal of the Knudsen number. For large Knudsen numbers, the curve is no longer linearity due to rarefaction.

For a given  $Kn$ , the gas density has to change inversely proportionally with the channel size. However, these kinds of changes will not affect the mixing coefficient. Fig. 8 shows the results for different channel sizes at a same Knudsen number value with the entering gas Mach number at 0.3.

### 3.6. Mach number effects

The Mach number effects on the micro gas mixing process are shown in Figs. 9 and 10. Fig. 9 shows that the dimensionless mixing coefficient increases nearly proportionally to the Mach number. Even through the temperature or velocity may vary, Fig. 10 shows that the dimensionless mixing

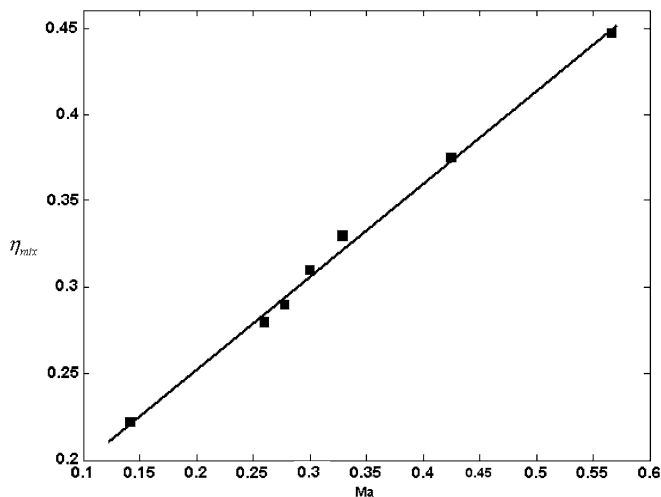


Fig. 9. Mixing coefficient variation for various Mach numbers at  $Kn = 0.1$ .

length does not change for a given Mach number with inlet temperature ( $Mach = 0.3$ ). The results validate the analysis of the relationships between the dimensionless mixing coefficient and the flow parameters.

## 4. Conclusions

The mixing behavior of gas flows in microchannels was investigated using the direct simulation Monte Carlo method. The simulation considered two parallel gas streams entering a microchannel with various wall characteristics, inlet velocities, gas temperatures and gas number densities.

The results show that the main flow velocity and temperature were the most important factors affecting the micro gas mixing. Although the wall characteristics do affect the velocity and temperature profiles, the effect on the mixing length is limited.

A dimensionless mixing coefficient, defined as the ratio of the mixing length to the channel height, was defined as proportional to the Mach number and inversely proportional to the Knudsen number. This result was validated for micro gas mixing flows, but is expected to apply to all laminar gas flows at all scales.

## Acknowledgement

The present work was supported by the National Natural Science Foundation of China (Grant No. 59995550-2).

## References

- [1] F.J. Alexander, A.L. Garcia, B.J. Alder, Cell size dependence of transport coefficients in stochastic particle algorithm, *Phys. Fluids* 10 (1998) 1540–1542.
- [2] F.J. Alexander, A.L. Garcia, B.J. Alder, Erratum: Cell size dependence of transport coefficients in stochastic particle algorithm [*Phys. Fluids* 10 1540 (1998)], *Phys. Fluids* 12 (2000) 731s.

- [3] G.A. Bird, *Molecular Gas Dynamics and the Direct Simulation of Gas Flows*, Clarendon, Oxford, 1994.
- [4] Y. Fang, W.W. Liou, Computations of the flow and heat transfer in microdevices using DSMC with implicit boundary conditions, *J. Heat Transfer* 124 (2002) 338–345.
- [5] B. Farouk, E.S. Oran, K. Kailasanath, Numerical simulation of the structure of supersonic shear layers, *Phys. Fluids A* 30 (11) (1991) 2786–2798.
- [6] M. Gad-el-Hak, The fluid mechanics of microdevices—the Freeman Scholar lecture, *J. Fluids Eng.* 121 (1999) 5–33.
- [7] A.L. Garcia, W. Wagner, Time step truncation error in direct simulation Monte Carlo, *Phys. Fluids* 12 (2000) 2621–2633.
- [8] C.M. Ho, Fluidics—the link between micro and nano sciences and technologies, in: *Technical Digest of the 14th IEEE International MEMS Conference*, Interlaken, Switzerland, 2001, pp. 375–384 (ISBN-0-7803-6251-9).
- [9] C.M. Ho, Y.C. Tai, Micro-electro-mechanical-systems (MEMS) and fluid flows, *Annu. Rev. Fluid Mech.* 30 (1998) 579–612.
- [10] N.G. Hadjiconstantinou, Analysis of discretization in the direct simulation Monte Carlo, *Phys. Fluids* 12 (2000) 2634–2638.
- [11] M. Ilgaz, M.C. Çelenligil, DSMC simulations of low-density choked flows in parallel-plate channels, in: *23rd International Symposium, AIP Conference Proceedings* 663 (2003) 831–840.
- [12] Y. Ju, C.W. Choi, An analysis of sub-limit flame dynamics using opposite propagating flames in mesoscale channels, *Combust. Flame* 133 (2003) 483–493.
- [13] G.E. Karniadakis, A. Beskok, *Micro Flows: Fundamentals and Simulation*, Springer, 2002.
- [14] W.W. Liou, Y. Fang, Heat transfer in microchannel devices using DSMC, *J. MicroElectroMech. Syst.* 10 (2001) 274–279.
- [15] F. Ochoa, C. Eastwood, P.D. Ronney, B. Dunn, Thermal transpiration based microscale propulsion and power generation devices, in: *7th International Workshop on Microgravity Combustion and Chemically Reacting Systems*, NASA/CP-2003-21376, June 2003.
- [16] D.J. Rader, M.A. Gallis, J.R. Torczynski, W. Wagner, DSMC convergence behavior for Fourier flow, in: *RGD24 International Symposium on Rarefied Gas Dynamics*, Bari, Italy, 2004.
- [17] M.A. Rieffel, A method for estimating the computational requirements of DSMC simulations, *J. Comput. Phys.* 149 (1999) 95–133.
- [18] H.A. Stone, A.D. Stroock, A. Ajdari, Engineering Flows in Small Devices: Microfluidics Toward a Lab-on-a-Chip, *Annu. Rev. Fluid Mech.* 36 (2004) 381–411.
- [19] M. Wang, Z.X. Li, Similarity of ideal gas flow at different scales, *Sci. China E* 46 (6) (2003) 661–670.
- [20] M. Wang, Z.X. Li, Non-ideal gas flow and heat transfer in micro and nano channels using the direct simulation Monte Carlo method, *Phys. Rev. E* 68 (2003) 046704.
- [21] M. Wang, Z.X. Li, Gas simulations for gas flows in microgeometries using the direct simulation Monte Carlo method, *Int. J. Heat Fluid Flow* 25 (6) (2004) 975–985.
- [22] M. Wang, Z.X. Li, Numerical simulations on performance of MEMS-based nozzles at moderate or low temperatures, *Microfluidics Nanofluidics* 1 (1) (2004) 62–70.
- [23] M. Wang, Z.X. Li, Micro and nano dense gas Poiseuille flow in a consistent Boltzmann algorithm model, *J. Micromech. Microeng.* 14 (7) (2004) 1057–1063.
- [24] M. Wang, Z.X. Li, Failure analysis of Molecular-Block model for the DSMC Method, *Phys. Fluids* 16 (6) (2004) 2122–2125.
- [25] M. Wang, Z.X. Li, Flow and heat transfer characteristics of dense gas in micro- and nanoscale channels, *Sci. China Ser. E* 48 (3) (2005) 317–325.
- [26] S. Watanabe, M.G. Mungal, Velocity fields in mixing-enhanced compressible shear layers, *J. Fluid Mech.* 522 (2005) 141–177.
- [27] F. Yan, B. Farouk, Numerical simulation of gas flow and mixing in a microchannel using the direct simulation Monte Carlo method, *Microscale Thermophys. Eng.* 6 (2002) 235–251.